

The Crystal Structures of Cavansite and Pentagonite¹

HOWARD T. EVANS, JR.

U.S. Geological Survey, Washington, D.C. 20244

Abstract

Cavansite and pentagonite, dimorphs of $\text{Ca}(\text{VO})(\text{Si}_4\text{O}_{10}) \cdot 4\text{H}_2\text{O}$ found in Malheur County, Oregon, are both orthorhombic and represent novel, layer-silicate structure types. Zigzag pyroxene-like $(\text{SiO}_3)_n$ chains, joined laterally into sheets parallel to the *a-c* plane, are present in both with tetrahedral apices pointed alternately plus and minus along the *b* axes. The lateral linkage in cavansite results in a network of 4-fold and 8-fold rings, but in pentagonite the network is entirely made up of 6-fold rings. The vanadyl groups VO^{2+} and Ca^{2+} ions lie in mirror planes between the silicate layers and are coordinated alternately to pairs of tetrahedral apices along the chains on opposite sides of the mirror planes. Vanadium is in square-pyramid coordination, and Ca is in 7-fold coordination in both structures. The H_2O molecules are poorly resolved, have high apparent thermal parameters, and are probably zeolitic. The special features of the structures favor twinning in pentagonite (commonly found in fiveling groups) but prohibit twinning in cavansite (in which twinning has not been observed). Refinement of the crystal structures (to $R = 0.109$ for cavansite, and $R = 0.081$ for pentagonite) gives bond lengths with estimated errors of ± 0.02 Å.

Discovery of Cavansite and Pentagonite

In 1960, an unusual blue mineral was found in a roadcut near Owyhee Dam, Malheur County, Oregon. Staples, Evans, and Lindsay (1968) found that this mineral consists of two polymorphs of the new compound $\text{Ca}(\text{VO})(\text{Si}_4\text{O}_{10}) \cdot 4\text{H}_2\text{O}$. These separate species were named cavansite and pentagonite, and their description and natural history are described in the preceding paper (Staples, Evans, and Lindsay, 1973). As often happens in such studies, a full understanding of the nature and chemistry of these two species was achieved mainly through crystal structure analysis. The results of a preliminary crystal chemical study were reported previously by Evans and Staples (1970). The structure analyses were carried out at the U.S. Geological Survey, and are described in detail in this paper.

Structure Determination of Cavansite

Buerger precession photographs of a prismatic crystal of cavansite showed it to be orthorhombic with space group symmetry $Pcmm$ or $Pc2_1n$. Powder diffraction and other crystallographic data have been given by Staples, Evans, and Lindsay (1973). The unit cell parameters given in Table 1 for cavansite and Table 4 for pentagonite are derived from single-

crystal diffractometer measurements on the crystals used for the final structure refinements. These differ slightly from those reported from X-ray powder data by Staples, Evans, and Lindsay (1973) who attribute such observed variations in cell parameters to changes in the amount of zeolitic water in the crystal structure, as affected by temperature and humidity.

For the structure analysis, X-ray intensities for 998 independent reflections were measured on a General Electric quarter-circle crystal orienter using Zr-filtered $\text{MoK}\alpha$ radiation. The intensities were measured manually, using a stationary-crystal, stationary-counter (peak-height) technique with two background measurements per reflection. These data included all those with Bragg angle less than 47° , and of these 361 were less than an arbitrarily chosen threshold value.

Without any other preliminary considerations (some earlier attempts to solve the structure from two-dimensional Patterson maps had been abandoned), the three-dimensional data were normalized (to obtain *E* values) and treated directly by the symbolic addition procedure of Karle and Karle (1966), on the assumption that the space group is centrosymmetric ($Pcmm$). The calculation was carried out on an IBM 360 Model 65 computer using XRAY67, the unified system for crystal structure computations of J. M. Stewart (1967). Using the termi-

¹ Publication authorized by the Director, U.S. Geological Survey.

TABLE 1. Structure and Thermal Parameters for Cavansite*

Atom	Type	x	y	z	$B, \text{\AA}$ (equiv.)	Thermal parameters ($\times 10^4$):					
						β_{11}	β_{22}	β_{33}	β_{12}	β_{13}	β_{23}
Ca	4(c)	0.0829(8)	0.25	0.3810(7)	1.53(10)	37(6)	25(3)	35(5)	0	5(6)	0
V	4(c)	0.4033(7)	0.25	0.5271(6)	1.54(9)	42(5)	22(3)	39(5)	0	-2(5)	0
Si ₁	8(d)	0.0954(7)	0.0336(5)	0.1839(6)	1.13(8)	24(5)	22(3)	23(5)	-2(3)	-10(5)	2(3)
Si ₂	8(d)	0.3165(6)	0.0431(5)	0.3925(6)	1.09(8)	24(5)	18(3)	26(5)	3(3)	-5(4)	-3(3)
O ₁	8(d)	0.0846(17)	0.1509(11)	0.1765(15)	1.3(2)	56(14)	12(6)	21(11)	2(9)	3(13)	-9(8)
O ₂	8(d)	0.2945(18)	0.1591(12)	0.4124(16)	1.9(3)	67(17)	25(8)	35(13)	-2(9)	-17(13)	-9(9)
O ₃	8(d)	0.4477(14)	0.0203(12)	0.2962(14)	1.3(2)	32(13)	28(8)	11(10)	-8(8)	6(10)	0(9)
O ₄	8(d)	0.1671(16)	-0.0118(11)	0.0423(14)	1.2(2)	41(14)	17(7)	18(11)	-9(8)	5(12)	-9(8)
O ₅	8(d)	0.1847(17)	-0.0062(13)	0.3176(16)	1.8(3)	53(15)	33(8)	20(12)	-14(10)	20(14)	6(9)
O ₆	4(c)	0.5515(25)	0.25	0.4570(32)	2.8(5)	37(22)	45(15)	101(33)	0	1(23)	0
O ₇ (H ₂ O)	8(d)	0.9471(22)	0.1186(16)	0.4700(24)	4.0(4)	118(26)	45(12)	113(25)	-40(14)	28(22)	1(15)
O ₈ (H ₂ O)	4(c)	0.3709(41)	0.25	0.1387(25)	4.6(8)	218(56)	68(21)	9(21)	0	112(27)	0
O ₉ (H ₂ O)	4(c)	0.8092(44)	0.25	0.2806(58)	8.4(1.2)	137(48)	116(33)	303(87)	0	117(60)	0

* Space group: $P6mm$ (D_{2h}^{16}). Unit cell: $a=9.792(2)\text{\AA}$, $b=13.644(3)\text{\AA}$, $c=9.629(2)\text{\AA}$; $Z=4$.

Standard errors indicated in parentheses in terms of last significant figures.

nology of this system, the following programs were linked together for the computation: DATRDN (raw data reduction); DATFIX (data normalization); SIGMA2 (search for hkl vector triplets); PHASE (symbolic addition procedure); FOURR (Fourier synthesis). The one-shot calculation was completely successful, requiring a total of 6 minutes of machine time (in actual fact, the last link was separated and carried out on a second night). The sharpened electron density map (E map) showed the structure in almost all its details. The silicate framework was clearly revealed, and the V and Ca atoms were sharply imaged on the mirror planes (with perhaps some question as to which was which), although the H₂O molecules were not so well resolved.

The initial model was refined by least squares analysis (using ORFLS; Stewart, 1967) and converged in four cycles to a structure that gave a conventional reliability index $R = 0.098$. While the postulated structure was thus proved, this result was not considered satisfactory, mainly because in the refinement of isotropic thermal parameters, B took on negative values for 10 of the 13 different atoms (all but the H₂O molecules). The excellent quality of the structure itself in terms of its electron density mapping and interatomic distances led to the conclusion that the anomalous thermal parameters resulted from systematic errors in the data measurements. Therefore a new crystal was selected and the data set remeasured on the Picker automatic diffractometer.

Careful diffractometer scans showed that any crystal of cavansite that is large enough for collecting reasonably good three-dimensional data is not

actually single, but a parallel group of two or more individuals deviating from perfect alignment with each other by 0.1 to 0.5 degree. This fact leads to severe fluctuations in the ratio of peak height to integrated intensity from reflection to reflection. The use of a θ - 2θ scanning technique with the Picker instrument was expected to overcome this difficulty. In this experiment, a crystal of dimensions $0.06 \times 0.08 \times 0.28$ mm was used to measure intensities of 1703 independent reflections (all with Bragg angles $< 60^\circ$), using Nb-filtered MoK α radiation. Of these, 903 had intensity values less than 3σ based on counting statistics for each reflection and were given zero weights in all subsequent calculations; the remaining 800 reflections were treated with unit weights. No corrections were made for absorption or extinction.

The new data set was analyzed by the least squares method using ORFLS, and in the final anisotropic modes a program (RFINE) written by L. W. Finger of the Geophysical Laboratory, Washington, D.C. Stable convergence of 34 structure (positional) and 68 thermal parameters was reached at $R = 0.109$. This time the thermal parameters (equivalent isotropic B values) varied from 1.1 to 2.8 \AA^2 for the cations and silicate framework, and 4.0 to 8.4 \AA^2 for the H₂O molecules, and were considered to be acceptable. The H₂O molecules have large and highly anisotropic thermal motions, and probably are not well represented by the structure factor functions assumed for them. A full least-squares cycle which included a variable population parameter for each H₂O molecule did not lead to any value for these parameters that was significantly different from unity.

TABLE 2. Calculated and Observed Structure Factors for Cavansite*

H	K	L	FO	FC	H	K	L	FO	FC	H	K	L	FO	FC	H	K	L	FO	FC	H	K	L	FO	FC	
0	2	0	48	72	8	2	1	18	25	1	4	3	15	-8	3	12	4	29	-30	1	14	0	34	36	
0	4	0	259	317	8	4	1	18	-12	1	12	1	76	78	3	16	4	23	-30	2	0	6	78	75	
0	0	0	179	-174	8	4	1	44	44	1	13	3	24	-24	4	1	4	19	8	2	3	6	90	53	
0	12	0	184	-135	8	4	1	36	35	1	19	3	60	56	3	4	6	-92	3	4	6	18	12		
0	0	0	89	-89	8	10	1	40	-34	1	17	3	42	-27	4	7	4	69	-60	2	7	6	32	35	
0	18	0	41	-36	8	13	1	20	19	2	1	3	35	-39	4	9	4	30	-28	2	10	6	35	-43	
1	1	0	136	-165	8	14	1	29	-29	2	2	5	82	91	5	0	6	96	-93	6	0	8	38	-25	
1	3	0	18	-19	9	2	1	31	-36	2	3	3	136	145	4	15	4	33	-15	3	1	6	52	-56	
1	5	0	70	-49	9	3	1	28	-26	2	4	3	88	-86	5	3	4	20	-28	3	2	6	63	-68	
1	7	0	60	-61	9	5	1	45	-44	2	5	3	21	56	5	5	4	32	-24	3	3	6	72	-74	
1	9	0	106	-102	9	6	1	15	-13	2	7	3	179	165	5	6	4	31	34	3	4	6	46	-48	
1	11	0	42	40	9	7	1	43	-39	2	8	3	79	-72	5	7	4	48	-47	3	5	6	33	-36	
1	13	0	35	39	9	8	1	16	15	3	9	3	30	31	5	2	4	21	-28	3	6	6	51	-50	
1	17	0	25	28	9	9	1	32	-36	2	11	1	72	65	6	5	4	15	20	3	7	6	46	-51	
1	19	0	49	46	10	0	1	22	20	2	12	1	57	-63	6	7	4	21	-21	3	8	6	66	-65	
2	0	0	56	53	10	2	1	28	27	3	13	1	39	40	6	8	4	22	23	3	9	6	63	-61	
2	2	0	74	-89	10	7	1	21	26	2	16	3	25	-34	6	10	4	28	23	3	10	6	41	52	
2	4	0	53	-45	11	0	1	51	45	3	17	3	32	-30	7	10	4	58	-62	3	12	6	16	-25	
2	6	0	74	-72	11	1	1	27	-23	3	18	3	71	-72	7	1	4	23	29	3	13	6	13	33	
2	8	0	15	-16	11	2	1	31	-29	3	1	3	45	-51	7	2	4	71	-76	3	16	6	22	-19	
2	10	0	74	-72	11	10	1	19	-24	3	2	3	18	-18	7	4	4	31	-34	4	0	6	58	-63	
3	1	0	120	-114	11	1	1	18	-25	3	3	3	62	-65	7	5	3	36	-40	7	2	6	43	-45	
3	3	0	32	33	12	4	1	19	-16	3	4	3	51	-51	7	4	4	53	-56	4	4	6	22	-28	
3	5	0	155	-166	12	5	1	45	-42	3	5	3	40	-42	7	8	4	25	-22	4	5	6	48	-49	
3	7	0	127	-129	12	7	1	38	-28	3	6	3	29	-24	7	9	4	24	25	4	6	6	40	-41	
3	11	0	19	26	10	0	2	43	38	3	7	3	72	-69	8	0	4	35	40	4	11	5	17	-14	
3	13	0	65	-64	10	0	2	80	69	3	8	3	74	-69	8	1	4	17	-21	5	2	6	64	64	
3	17	0	29	-31	10	2	1	18	-19	3	9	3	48	-45	8	2	4	32	-24	5	3	6	51	-52	
4	0	0	138	-152	10	0	2	22	-14	3	10	3	42	-42	9	0	4	51	-48	5	7	5	16	-19	
4	2	0	14	15	10	0	2	55	58	3	12	4	36	-39	9	1	4	40	-22	5	8	6	21	-22	
4	4	0	108	-119	10	0	2	103	-96	3	13	4	33	-35	9	2	4	37	-32	5	9	6	16	-17	
4	6	0	44	37	10	0	2	51	53	4	1	3	113	-114	9	5	4	17	-25	6	5	6	72	-69	
4	8	0	57	-52	10	0	2	21	25	4	1	3	41	-44	9	6	4	18	-18	6	1	6	55	-59	
4	10	0	32	34	10	0	2	76	-73	4	1	3	23	-23	9	7	4	16	-22	6	2	6	45	-49	
4	14	0	9	9	10	0	2	11	20	-16	4	1	3	45	46	9	8	4	20	-24	6	3	6	54	-56
4	16	0	27	-28	10	0	2	35	39	4	1	3	64	-69	10	0	4	22	27	6	4	6	39	-41	
5	1	0	26	-24	10	0	2	15	12	-11	5	2	32	-31	10	0	4	32	-31	6	5	6	33	-39	
5	3	0	74	-72	10	0	2	35	42	4	7	3	71	65	10	3	4	45	45	6	6	6	37	41	
5	5	0	109	-114	10	0	2	70	70	4	10	3	75	69	10	7	4	67	62	6	10	6	47	47	
5	7	0	17	-17	1	1	2	40	-41	4	11	3	31	23	10	9	4	30	-35	6	12	6	29	24	
5	9	0	58	-60	1	1	2	35	42	4	14	3	29	33	12	1	4	23	0	6	13	6	33	38	
5	11	0	50	-51	1	1	2	51	56	4	16	3	34	34	12	1	4	23	0	6	14	6	20	24	
5	13	0	61	61	1	1	2	37	39	4	18	3	39	34	13	2	4	29	27	7	1	5	32	34	
5	15	0	25	-27	1	1	6	22	-22	5	1	3	85	86	1	10	5	110	111	7	2	5	23	22	
5	17	0	53	-51	1	1	6	25	-25	5	1	3	85	86	1	12	5	22	-24	7	3	4	23	31	
5	19	0	72	76	1	1	8	25	-25	5	3	3	18	-25	1	4	5	99	99	7	5	0	42	42	
5	21	0	33	33	1	1	10	25	-25	5	4	3	13	-21	1	6	5	17	-17	7	7	0	46	46	
5	23	0	83	83	1	1	2	84	84	5	5	3	94	94	1	7	6	46	46	7	9	0	35	6	
5	25	0	85	-86	2	1	2	26	-26	5	6	3	115	108	1	8	5	58	54	7	9	0	51	45	
5	27	0	49	51	2	1	2	91	-98	5	7	3	35	33	1	10	5	41	-45	7	12	6	10	28	
5	29	0	128	-133	2	1	2	86	-85	5	10	3	35	30	1	11	5	19	-29	7	14	6	18	22	
5	31	0	44	-51	2	1	2	48	-46	5	12	3	30	-33	2	1	5	80	-83	8	5	6	17	22	
5	33	0	83	-81	2	1	2	41	37	5	13	3	36	37	2	2	5	24	31	8	7	6	20	15	
5	35	0	29	-20	2	1	2	16	-23	5	14	3	22	24	2	4	5	51	-55	9	0	6	71	78	
5	37	0	11	14	2	1	2	19	-5	5	15	3	19	-2	2	3	5	57	-62	9	1	6	20	23	
5	39	0	77	78	2	1	6	21	24	3	16	3	31	-38	2	4	6	38	40	9	2	6	38	40	
5	41	0	21	21	3	0	2	123	-129	3	0	3	30	34	2	7	5	50	38	9	4	6	41	47	
5	43	0	80	75	3	1	2	38	32	6	1	3	19	24	2	7	5	30	24	9	5	6	40	46	
5	45	0	93	83	3	1	2	38	32	6	1	3	34	-34	2	8	5	76	-74	10	0	6	30	-40	
5	47	0	45	-47	3	1	2	106	111	6	1	3	35	36	2	13	5	45	-46	10	2	6	27	10	
5	49	0	68	-69	3	1	2	25	24	6	4	3	17	19	2	13	5	34	-30	10	5	6	27	10	
5	51	0	48	-50	3	1	2	18	-22	6	4	3	18	-23	3	0	10	1	18	-16	10	5	6	47	-50
5	53	0	91	92	3	1	2	62	-59	7	0	3	32	28	3	1	5	13	17	12	1	6	24	-28	
5	55	0	11	-11	3	1	2	50	45	7	2	3	61	62	3	2	5	56	64	1	0	7	35	-41	
5	57	0	40	-34	3	1	2	37	31	7	3	3	84	-85	3	2	5	32	-31	1	1	7	35	-41	
5	59	0	64	-61	3	1	2	34	37	7	4	3	19	-22	3	4	5	34	35	3	3	7	50	-49	
5	61	0	107	-107	3	1	2	47	50	7	4	3	22	23	3	4	5	34	35	3	3	7	50	-49	
5	63	0	18	-18	3	1	2	28	31	7	5	3	53	52	3	5	5	29	34	3	4	7	10	-74	
5	65	0	39	37	3	1	2	21	26	7	7	3	40	-38	3	6	5	15	-19	3	5	7	31	6	
5	67	0	116	-117	3	1	2	36	33	7	8	3	35	-37	3	7	5	15	-19	3	6	7	31	6	
5	69	0	104	104	3	1	2	36	-30	7	10	3	25	2	4	0	5	45	-48	3	7	7	70	-78	
5	71	0	29	28	3	1	2	38	35	7	12	3	33	-29	4	1	5	93	-99	4	7	7	70	-74	
5	73	0																							

Also, an attempt was made to represent O_B as two half-atoms separated by about 0.5\AA , but this procedure also led to no significant new result. The final results based on the best refinement of 103 parameters (including one scale factor) are listed in Table 1. The list of observed and calculated structure amplitudes is given in Table 2.

The anisotropic thermal parameters given in Table 1 are transformed to the parameters of dimensions (root-mean-square vibrations in \AA) and orientations of principal ellipsoid axes, which are set forth in Table 3. These ellipsoids are visible in the stereoscopic view of the structure in Figure 5.

Determination of the Structure of Pentagonite

In the case of pentagonite, twinning was the greatest obstacle to what might otherwise have been a straightforward structure analysis. At first, no crystals of suitable size could be found that did not consist of 3 to 5 twin components, and physical separation of these did not seem to be practical. The measurement of three-dimensional data from such crystals with the Picker diffractometer was not possible. A three-dimensional data set was therefore first collected from Buerger precession photographs of 14 different nets in the pentagonite lattice. The crystal used was approximately $0.05 \times 0.1 \times 0.2$ mm in overall dimensions, but contained deep re-entrant angles. It consisted of three twin components having volume ratios of approximately 1:2:2. The nets recorded for one of the stronger components were: $0kl$, $1kl$, $2kl$, $h0l$, $h1l$, $h2l$, $h3l$, hhl , $h(h+2)l$, $h(h+4)l$, $h3h1$, $h(3h+2)l$, $h(3h+4)l$, $hk0$. The

patterns were recorded on Ilford Type G film, using $\text{MoK}\alpha$ radiation, which would make accessible about 1,050 independent reflections with Bragg angles $< 50^\circ$. Of these, 565 were measured by visual comparison with a calibrated strip, 266 were too weak to measure, and the remainder were not registered on the available nets. The observed intensities were corrected for Lorentz and polarization effects by the method and charts of Burbank (1952). They were then reduced to a common scale by an empirical comparative process making use of the reflections common to the various nets. The resulting data set formed the basis of the earlier stages of the structure analysis.

Before the film-measured, three-dimensional data set became available, considerable effort was applied to a reasoned deduction of a probable structure based on the space group $Ccmm$ (assumed at this stage to be centrosymmetric), the dimensions of the unit cell (Table 4), and the known structure of the obviously closely related cavansite. It seemed certain that a silicate layer structure must be involved, and that the layers must be held together by the cations lying in mirror planes between the layers in some very similar fashion. The key was sought in some variation of the tetrahedral linkage in the silicate layer. Without trying to reconstruct the reasoning that led to the correct solution, it may simply be stated that the 4-8 ring network of cavansite could not by any means be fitted into the pentagonite unit cell, but that the silicate chains must be assembled differently into 6-fold rings. The c/a ratios of cavansite and pentagonite ($0.983 \sim 1$ and $0.863 \sim \sqrt{3}/2$, respectively) tended to confirm this conclusion. Then, by placing VO^{2+} and Ca^{2+} ions on 2-fold axes in the interlayer mirror planes (required for VO^{2+} in space group $Ccmm$), a structure was obtained that fitted the cell geometry very neatly and had quite satisfactory crystal chemical properties. This model was tested with three sets of two-dimensional data ($hk0$, $h0l$, $0kl$). The electron density projection confirmed the proposed structure fairly well, but the consolidated data on least squares refinement would not yield a reliability index better than $R = 0.29$, and no information could be gained about the location of the H_2O molecules. Nevertheless, at this stage the general principles of the silicate framework were felt to be unequivocally established.

Turning to the three-dimensional data, the derived model (excluding H_2O molecules) was tested by one cycle of least squares analysis and an electron density

TABLE 3. Dimensions and Orientations of Thermal Ellipsoids in Cavansite*

Atom	Rms vib.	Angle to a	Angle to b	Angle to c	Atom	Rms vib.	Angle to a	Angle to b	Angle to c
O_8	0.121(12)	125(24)	90	35(24)	O_4	0.07(4)	86(26)	59(22)	31(25)
	0.140(12)	145(24)	90	125(24)		0.12(3)	152(23)	112(21)	106(27)
	0.153(10)	90	0	90		0.16(2)	45(24)	129(21)	72(17)
V	0.133(9)	70(90)	90	20(90)	O_5	0.06(5)	118(12)	105(11)	32(13)
	0.143(14)	90	0	90		0.16(3)	129(23)	125(25)	121(14)
	0.143(14)	160(90)	0	70(90)		0.20(2)	51(21)	141(24)	84(17)
Si_1	0.080(16)	48(10)	89(9)	42(10)	O_6	0.13(4)	0(22)	90	90(22)
	0.123(11)	46(13)	70(20)	129(12)		0.21(4)	90	0	90
	0.147(9)	105(16)	20(20)	78(14)		0.22(4)	90(22)	90	0(22)
Si_2	0.096(13)	39(26)	92(22)	51(27)	O_7	0.14(3)	128(9)	137(11)	75(15)
	0.112(12)	59(30)	122(17)	132(29)		0.23(3)	83(18)	114(18)	155(19)
	0.140(10)	111(14)	147(16)	67(14)		0.29(3)	39(9)	122(12)	70(20)
O_1	0.07(4)	95(15)	51(19)	40(19)	O_8	0.06(8)	87(7)	90	3(7)
	0.13(3)	91(35)	40(20)	130(19)		0.25(4)	90	0	90
	0.17(2)	6(16)	86(28)	87(26)		0.33(4)	3(7)	90	87(7)
O_2	0.10(3)	71(14)	66(20)	32(16)	O_9	0.19(5)	152(10)	90	62(10)
	0.16(2)	104(38)	25(22)	110(25)		0.33(5)	90	0	90
	0.19(2)	155(26)	96(37)	66(19)		0.41(6)	62(10)	90	28(10)
O_3	0.07(4)	86(26)	59(22)	31(25)					
	0.12(3)	45(25)	54(27)	114(31)					
	0.17(2)	67(21)	157(21)	88(14)					

*Principal vibrations (root-mean-square) in \AA cited for each atom; angles in degrees. Standard errors indicated in parentheses in terms of last significant figures.

synthesis. The silicate framework was clearly resolved, and two strong peaks appeared for Ca and V, but no other sensible features emerged. Various arrangements of V and Ca on the 2-fold axis, and of H₂O molecules, led to a reliability index no lower than 0.40. An attempt at this stage to use the symbolic addition procedure did not lead to any possible alternative solution. Then it was noticed that in all of the several three-dimensional electron density maps, a moderate peak persisted in the mirror plane ($y = 0$) at $x = -0.017$, $z = 0.058$. This site would permit satisfactory coordination of vanadium to a pair of SiO₄ tetrahedral apices from each of the adjacent silicate sheets, but such an assignment requires a shift to the noncentrosymmetric space group *Ccm2*₁. A least squares analysis on this model led to rapid convergence to $R = 0.200$, and resolution of all the remaining oxygen atoms.

At this stage a new specimen, which carried both cavansite and pentagonite in crystals of superior quality, was obtained from the National Museum (no. 120584). From this a few excellent, untwinned crystals of pentagonite could be obtained and a crystal of dimensions of $0.06 \times 0.07 \times 0.23$ mm was used to measure 1,010 reflections with $2\theta < 60^\circ$ in the same manner as with cavansite. Of these, 419 had intensities less than 3σ in terms of counting statistics, and were excluded from subsequent calculations. No corrections were made for absorption or extinction.

Refinement of the existing model converged smoothly to a final reliability index $R = 0.081$, in full anisotropic mode based on 102 parameters (including one scale factor). In the last stages, corrections for anomalous dispersion were included. The

results are shown in Table 4, and the observed and calculated structure factors are given in Table 5. The dimensions and orientations of the thermal parameters are given in Table 6. In the last cycles O₅ actually became nonpositive definite, but not significantly so, and the β_{13} , β_{23} and β_{33} terms for this atom in Table 4 have been changed from the computer result by a maximum of about 1.2 standard deviations to avoid this condition. Since no absorption or extinction corrections have been made, this change does not seem unreasonable. The water molecule O₉ is very diffuse, but an attempt to refine population parameters for this and also O₇ and O₈ did not indicate any significant departure from full occupancy.

In the refinement by the Finger program, anomalous dispersion for V, Ca and Si was included in the structure factor function. When the least squares analysis was completed, the parameters z , β_{13} and β_{23} were replaced by their negative values for all atoms and the refinement repeated. The results of the two refinements were not significantly different from each other in terms of the residuals ($R = 0.081$ for both). In terms of parameters, z_V shifted by 0.03 \AA ($\sim 5\sigma$) and z_{Ca} shifted by $.02 \text{ \AA}$ ($\sim 2.5\sigma$), while changes in all other parameters, including thermal parameters, were less than 0.6σ . In terms of bond lengths, the only bond seriously affected was V-O₆, which changed from 1.565 to 1.540 \AA ($\Delta \sim 1.1\sigma$). The results of the first refinement are cited in the tables. The standard deviations of z for Ca and V shown in Table 4 have been estimated to reflect the additional uncertainty resulting from anomalous dispersion effects mentioned above.

TABLE 4. Structure and Thermal Parameters for Pentagonite*

Atom	Type	x	y	z	B, \AA^2 (equiv.)	Thermal parameters ($\times 10^4$):					
						β_{11}	β_{22}	β_{33}	β_{12}	β_{13}	β_{23}
Ca	4(a)	0.2403(5)	0.0	0.2674(20)	1.38(8)	38(4)	19(2)	33(5)	0	8(7)	0
V	4(a)	-0.0224(4)	0.0	0.0553(30)	1.36(8)	35(4)	16(2)	43(5)	0	-11(4)	0
Si ₁	8(b)	0.1272(6)	0.2062(4)	0.0871(7)	1.11(10)	37(6)	15(3)	17(7)	-1(3)	-2(5)	0(3)
Si ₂	8(b)	0.1232(6)	0.2074(4)	0.4265(8)	0.85(9)	14(4)	9(3)	38(7)	-1(9)	-9(5)	2(4)
O ₁	8(b)	0.1231(15)	0.0927(10)	0.0842(19)	1.5(3)	41(14)	9(7)	59(24)	-1(9)	21(16)	7(9)
O ₂	8(b)	0.1201(16)	0.0934(10)	0.4358(17)	1.1(2)	34(13)	13(7)	30(19)	7(9)	6(14)	-6(9)
O ₃	8(b)	0.2532(18)	0.2468(19)	0.0115(18)	1.8(2)	26(10)	22(6)	81(16)	-15(6)	3(11)	4(9)
O ₄	8(b)	0.0036(19)	0.2540(8)	0.0075(18)	1.6(2)	31(11)	13(5)	83(16)	-2(11)	-25(11)	9(12)
O ₅	8(b)	0.1229(13)	0.2455(9)	0.2573(18)	1.5(2)	52(9)	25(5)	18(16)	4(12)	6(14)	16(13)
O ₆	4(a)	-0.0887(22)	0.0	0.2136(24)	2.5(4)	59(22)	46(14)	49(25)	0	8(19)	0
O ₇ (H ₂ O)	8(b)	0.3968(20)	0.1188(12)	0.2425(27)	4.0(7)	121(27)	48(11)	99(33)	-22(13)	-57(25)	35(17)
O ₈ (H ₂ O)	4(a)	0.6250(34)	0.0	-0.0035(33)	4.8(1.1)	130(40)	69(24)	112(49)	0	-79(37)	0
O ₉ (H ₂ O)	4(a)	0.353(5)	0.0	-0.096(12)	14.8(4.0)	98(53)	133(52)	94(33)	0	124(90)	0

* Space group: *Ccm2*₁ (*C*_{2v}¹²). Unit cell: $a=10.386(4)\text{\AA}$, $b=14.046(7)\text{\AA}$, $c=8.975(3)\text{\AA}$; $Z=4$.

Standard errors indicated in parentheses in terms of last significant figures.

TABLE 5. Calculated and Observed Structure Factors for Pentagonite*

H	K	L	FO	FC	AC	BC	H	K	L	FO	FC	AC	BC	H	K	L	FO	FC	AC	BC	H	K	L	FO	FC	AC	BC
0 0 2	186	177	166	60			1 11 10	16	-14	-8	2 18 5	25	26	26	2	4 2 9	8	1	8	5 9 1	19	23	11	-20			
0 0 4	166	158	144	85			1 13 0	22	22	1	2 16 6	35	25	4	24	4 2 10	44	49	-32	-36	5 9 2	28	29	-24	16		
0 0 6	210	207	-87	-1			1 13 1	12	-9	21	2 16 7	5	1	5		4 2 11	11	-10	5	5 9 3	9	92	91	15			
0 0 8	38	36	-35	4			1 13 2	16	22	-9	2 18 0	0	0	0		4 2 12	36	38	32	21	5 9 4	41	49	30	39		
0 0 10	20	-12	-14				1 13 3	35	41	40	2 18 1	9	18	-8	-8	4 4 0	114	111	111	2	5 9 5	5	29	29	1		
0 0 12	87	78	45	44			1 13 4	20	26	17	2 18 2	2	30	24	17	4 4 1	26	31	25	-19	5 9 6	8	27	32	22		
0 0 2 4	57	-57	-2				1 13 5	8	12	-9	3 1 10	42	43	23	-27	4 4 2	68	83	52	37	5 9 7	7	18	25	5		
0 0 2 2	109	109	-107	19			1 13 6	22	29	-12	2 18 4	0	15	-12	10	4 4 3	21	25	23	-11	5 9 8	8	22	13	17		
0 0 2 4	41	46	17	43			1 13 7	17	8	15	3 1 10	14	14	1	4	4 4 4	105	106	77	72	5 9 9	9	34	35	-32		
0 0 2 6	38	40	15	37			1 13 8	9	-9	0	3 1 10	42	43	23	-27	4 4 5	15	26	23	12	5 9 10	10	27	-21	-17		
0 0 2 8	34	26	-15	21			1 13 9	26	-22	-13	3 1 10	26	27	21	17	4 4 6	25	28	15	23	5 11 0	0	25	25	1		
0 0 2 10	55	53	-1	-1			1 13 10	58	55	2	3 1 10	100	96	-84	-46	4 4 7	33	16	8	15	5 11 1	1	28	13	-26		
0 0 2 12	73	65	-58	-29			1 15 1	28	31	-29	-12	3 1 10	42	43	23	-27	4 4 8	31	38	15	5	5 11 2	2	18	17	0	
0 0 4 0	301	320	320	4			1 15 2	43	39	35	19	3 1 10	5	9	8	4	4 4 9	23	22	5	-21	5 11 3	3	53	52	3	
0 0 4 2	88	92	87	28			1 15 3	6	-6	-21	3 1 10	7	6	-5	-5	4 4 10	31	23	-20	-11	5 11 4	4	28	29	17		
0 0 4 4	152	154	124	89			1 15 4	24	22	-6	21	3 1 10	7	6	-5	-5	4 4 11	23	20	-2	10	5 11 5	5	53	52	3	
0 0 4 6	40	43	-37	21			1 15 5	5	27	-20	-17	3 1 10	8	17	17	-10	4 4 12	31	28	-20	-11	5 11 6	6	17	-2	17	
0 0 4 8	37	42	9	41			1 15 6	24	-25	15	3	3 1 10	9	55	48	27	40	4 4 13	36	32	-24	5	5 11 7	7	24	25	25
0 0 4 10	27	28	22	18			1 15 7	25	19	18	3	3 1 10	7	25	19	-12	4 4 14	48	49	-88	13	5 11 8	8	14	14	1	
0 0 4 12	32	31	-31	3			1 15 8	8	27	-27	4	3 1 11	22	10	8	-5	4 4 15	3	19	20	-14	5 11 9	9	15	-14	-5	
0 0 6 0	70	68	-66	15			1 17 0	6	6	0	3 3 10	168	169	-18	-25	4 4 16	49	45	1	45	5 11 10	10	23	23	0		
0 0 6 2	46	50	-12	49			1 17 1	1	6	0	3 3 10	168	169	-18	-25	4 4 17	25	30	30	0	5 11 11	11	25	-10	-17		
0 0 6 4	33	33	-24	22			1 17 2	21	26	-22	13	3 3 10	160	158	156	-23	4 4 18	108	107	-105	-20	5 11 12	12	19	19	0	
0 0 6 6	31	32	87	28			1 17 3	80	76	66	13	3 3 10	127	128	124	34	4 4 19	30	32	-26	18	5 11 13	13	13	13	4	
0 0 6 8	10	24	34	-17	-29		1 17 4	27	27	17	21	3 3 10	25	25	25	10	4 4 20	8	10	10	10	5 11 14	14	10	10	22	
0 0 6 10	12	20	29	-23	12		1 17 5	5	13	13	0	3 3 10	50	47	-30	36	4 4 21	11	11	11	11	5 11 15	15	6	6	-5	
0 0 6 12	30	29	-32	17			1 17 6	39	36	25	25	3 3 10	103	100	107	14	4 4 22	55	60	-51	-32	5 11 16	16	18	18	0	
0 0 8 0	171	167	167	6			1 19 0	50	54	54	1	3 3 10	66	66	66	10	4 4 23	11	11	-13	-2	5 11 17	17	3	3	28	
0 0 8 2	36	34	-32	22			1 19 1	29	28	-12	3	3 3 10	35	34	-38	-8	4 4 24	131	131	131	3	5 11 18	18	9	9	-10	
0 0 8 4	168	165	152	63			1 19 2	28	-15	-12	3	3 3 10	35	34	-38	-8	4 4 25	131	131	131	3	5 11 19	19	10	10	0	
0 0 8 6	41	38	32	31			1 19 3	11	8	35	49	3 3 10	12	15	-53	-9	4 4 26	104	104	104	27	5 11 20	20	16	16	-10	
0 0 8 8	63	70	52	46			1 19 4	18	-18	-2	3	3 3 10	28	23	-23	5	4 4 27	104	104	101	27	5 11 21	21	10	10	0	
0 0 8 10	42	43	-38	-21			2 2 0	0	38	35	35	0	3 1 10	3	-2	-1	4	4 4 28	2	0	-2	2	5 11 22	22	12	12	2
0 0 8 12	181	182	182	1			2 2 0	1	127	132	-132	-133	3 1 10	40	30	-30	-11	4 4 29	48	2	0	-2	5 11 23	23	13	13	4
0 0 10 0	58	53	44	28			2 2 0	2	106	116	93	69	3 3 12	23	16	-11	11	4 4 30	48	2	0	-2	5 11 24	24	58	53	24
0 0 10 2	51	59	-52	18			2 2 0	3	216	226	-226	1	3 5 0	5	0	0	4	4 4 31	48	2	0	-2	5 11 25	25	11	11	0
0 0 10 4	141	137	138	26			2 2 0	1	124	117	116	16	3 5 0	88	83	75	-35	4 4 32	48	2	0	-2	5 11 26	26	31	31	4
0 0 10 6	91	84	-82	-18			2 2 0	5	108	109	-101	-37	3 5 2	51	51	46	-23	4 4 33	48	2	0	-2	5 11 27	27	61	61	1
0 0 10 8	2	3	-5	-12			2 2 0	6	67	66	0	66	3 5 3	89	89	-85	-27	4 4 34	48	2	0	-2	5 11 28	28	11	11	0
0 0 10 10	46	46	46	4			2 2 0	7	78	78	78	69	3 5 3	78	78	78	69	4 4 35	48	2	0	-2	5 11 29	29	11	11	0
0 0 10 12	13	-7	-21	2			2 2 0	8	59	50	-46	-19	3 5 3	35	41	18	38	4 4 36	48	2	0	-2	5 11 30	30	22	22	-2
0 0 12 0	107	106	90	35			2 2 0	9	83	84	73	37	3 5 6	52	54	42	33	4 4 37	48	2	0	-2	5 11 31	31	16	16	6
0 0 12 2	33	40	30	57			2 2 0	10	34	28	-21	18	3 5 8	17	-11	12	12	4 4 38	48	2	0	-2	5 11 32	32	17	17	0
0 0 12 4	40	40	30	57			2 2 0	11	73	74	55	50	3 5 8	17	-11	12	12	4 4 39	48	2	0	-2	5 11 33	33	17	17	0
0 0 12 6	41	41	-23	-9			2 2 0	12	35	35	-11	-33	3 5 9	48	51	40	32	4 4 40	48	2	0	-2	5 11 34	34	17	17	0
0 0 12 8	81	77	17	15			2 2 0	13	114	121	-13	0	3 5 11	21	26	-26	-1	4 4 41	48	2	0	-2	5 11 35	35	17	17	0
0 0 12 10	24	18	15	9			2 2 0	14	41	46	-30	34	3 7 0	172	173	173	2	4 4 42	48	2	0	-2	5 11 36	36	17	17	0
0 0 12 12	33	42	-25	19			2 2 0	15	120	124	100	76	3 7 0	111	108	111	4	4 4 43	48	2	0	-2	5 11 37	37	17	17	0
0 0 14 0	88	87	69	42			2 2 2	1	59	49	-42	-10	3 7 2	105	104	99	34	4 4 44	48	2	0	-2	5 11 38	38	17	17	0
0 0 14 2	44	47	-27	14			2 2 2	2	43	45	-43	13	3 7 3	72	77	77	-0	4 4 45	48	2	0	-2	5 11 39	39	17	17	0
0 0 14 4	33	30	30	2			2 2 2	3	85	88	87	17	3 7 3	60	58	-2	31	4 4 46	48	2	0	-2	5 11 40	40	17	17	0
0 0 14 6	63	63	63	6			2 2 2	4	61	68	4	68	3 7 3	93	96	94	19	4 4 47	48	2	0	-2	5 11 41	41	17	17	0
0 0 14 8	73	73	61	40			2 2 2	5	50	49	-48	-12	3 7 6	76	83	-82	9	4 4 48	48	2	0	-2	5 11 42	42	17	17	0
0 0 14 10	24	14	19	9			2 2 2	6	46	45	-10	20	3 7 6	49	45	-10	20	4 4 49	48	2	0	-2	5 11 43	43	17	17	0
0 0 14 12	23	-23	5	5			2 2 2	7	50	54	-52	-12	3 7 6	50	54	-52	-12	4 4 50	48	2	0	-2	5 11 44	44	17	17	0
0 0 16 0	48	48	48	4			2 2 2	8	42	36	-34	-12	3 7 9	35	37	-37	-1	4 4 51	48	2	0	-2	5 11 45	45	17	17	0
0 0 16 2	133	156	150	63			2 2 4	0	8	2	2	0	3 7 11	45	41	-34	-23	4 4 52	48	2	0	-2	5 11 46	46	17	17	0
0 0 16 4	109	118	-115	-26			2 2 4	1	84	-78	-18	-18	3 9 0	23	26	-26	-1	4 4 53	48	2	0	-2	5 11 47	47	17	17	0
0 0 16 6	115	118	94																								

TABLE 5, continued

H	K	L	FO	FC	AC	BC	H	E	L	FO	FC	AC	BC	H	E	L	FO	FC	AC	BC	H	K	L	FO	FC	AC	BC	H	K	L	FO	FC	AC	BC	
6 18	3		23	-20	-12		7 17	1		15	0	-19		8 1	1	49	40	-27	-25		15	2	8	12	-10	-6		11	9	4		5	5	-2	
6 18	4		11	-11	1		7 17	2		12	-11	4		8 1	2	26	14	14	-11		15	2	9	32	-32	-10		11	10	5		12	5	-12	
6 18	5		6	-9	1		8 1	2	255	233	123	3		9 1	3	43	25	21	-13		10	4	0	18	-18	-10		11	11	6		34	25	11	
6 18	6		0	-6	0		9 1	4		18	11	-14		9 1	4	4	4	-2	7		13	4	1	37	38	-24	-29	11	11	0		11	11	-11	
7 1	1	35	34	0	0		9 1	5		8	8	3		9 1	5	13	-7	-11	10		13	4	2	31	38	-24	-29	11	11	0		21	18	-11	
7 1	1	82	77	74	-19		9 1	6		31	34	31	-14	9 1	6	37	34	-15	-8		14	4	2	26	31	19	8	11	11	2		4	4	0	
7 1	2	57	55	51	29		9 1	7		4	30	33	21	9 1	7	36	39	27	28		15	4	4	14	-10	-10		11	11	3		11	1	-1	
7 1	3	47	44	41	-10		9 1	8		5	49	45	41	9 1	8	19	-19	3	3		15	4	5	8	-5	-3		11	11	4		6	-3	-5	
7 1	4	32	32	-26	18		9 1	9		106	105	-194	-31	9 1	9	0	0	11	10		15	4	6	20	14	4		11	11	5		9	4	0	
7 1	5	86	84	77	32		9 1	10		15	15	1		9 1	10	57	-17	0	0		15	4	7	43	48	37	30	12	0	0		58	53	-93	
7 1	6	22	22	-26	11		9 1	11		29	-19	14		9 1	11	36	30	8	-28		15	4	8	12	-8	-9		12	0	1		33	31	23	
7 1	7	32	33	-13	-1		9 1	12		22	26	17	25	9 1	12	33	37	3	8		15	4	9	24	-23	-10		12	0	2		26	34	-34	
7 1	8	27	27	-13	-1		9 1	13		10	10	7	-7	9 1	13	101	96	96	-5		15	4	10	27	24	12	-21	42	0	3		10	1	-9	
7 1	9	26	26	-8	24		9 1	14		76	77	-77	0	9 1	14	38	38	31	22		15	4	11	19	14	13		12	0	4		43	51	48	
7 1	10		3	-3	5		9 1	15		52	47	14	-45	9 1	15	0	0	0	0		15	4	12	10	-10	-10		12	0	5		25	27	20	
7 1	11	39	33	-11	-10		9 1	16		3	56	59	-59	-59	-59	-59	-59	-59	-59		15	4	13	10	-10	-10		12	0	6		74	70	21	
7 1	12	75	73	-23	-0		9 1	17		3	31	38	23	-30	9 1	17	21	1	24		15	4	14	16	25	8		12	0	7		5	25	27	
7 1	13	19	27	1	-27		9 1	18		2	26	26	12	23	9 1	18	26	21	16		15	4	15	16	8	14		12	0	8		46	45	1	
7 1	14	3	15	0	15		9 1	19		2	5	37	37	32	18	9 1	19	33	-33	-2		15	4	16	8	14		12	0	9		26	22	-14	
7 1	15	51	53	-40	-25		9 1	20		2	27	27	29	24	9 1	20	61	58	58	13		15	4	17	8	-5	-15		12	0	10		26	-23	-14
7 1	16	24	24	10	27		9 1	21		7	7	7	6	9 1	21	46	46	-37	-27		15	4	18	8	-5	-15		12	0	11		13	3	-12	
7 1	17	5	28	16	27		9 1	22		2	9	16	16	9 1	22	5	-1	-5	-5		15	4	19	12	18	7	-16		12	0	12		18	-15	-10
7 1	18	55	53	46	26		9 1	23		10	26	28	0	21	9 1	23	15	-9	-11		15	4	20	16	12	2	5		12	0	13		27	27	-0
7 1	19	3	15	13	9		9 1	24		10	26	32	-21	9 1	24	0	0	0	0		15	4	21	16	73	-73	-73		12	0	14		70	63	-56
7 1	20	16	16	0	16		9 1	25		11	11	11	2	9 1	25	16	-15	-1	-1		15	4	22	8	7	-3		12	0	15		2	2	0	
7 1	21	60	60	-30	52		9 1	26		11	30	33	26	-21	9 1	26	45	45	-45	-7		15	4	23	19	21		12	0	16		9	9	0	
7 1	22	36	37	37	1		9 1	27		12	26	28	1	9 1	27	44	43	36	22		15	4	24	19	17	16		12	0	17		23	18	-14	
7 1	23	1	46	50	48	-11	9 1	28		13	12	8	-9	9 1	28	10	9	3	3		15	4	25	24	19	17		12	0	18		0	0	0	
7 1	24	56	54	47	18		9 1	29		14	66	59	52	27	9 1	29	25	14	11		15	4	26	24	19	17		12	0	19		14	11	-9	
7 1	25	3	53	51	47	-18	9 1	30		15	40	47	41	21	-21	-21	0	0	0		15	4	27	41	-41	-30	-2	12	0	20		4	27	29	11
7 1	26	36	39	-34	20		9 1	31		16	32	34	28	18	9 1	31	103	95	95	-0		15	4	28	41	-41	-18		12	0	21		26	22	14
7 1	27	5	56	56	7	0	9 1	32		17	24	24	10	-10	9 1	32	33	39	29	26		15	4	29	41	-41	-18		12	0	22		24	2	2
7 1	28	6	38	41	-39	10	9 1	33		18	24	24	10	-10	9 1	33	33	39	29	26		15	4	30	41	-41	-18		12	0	23		10	10	0
7 1	29	16	-14	-6	0		9 1	34		19	23	24	14	20	9 1	34	33	39	29	26		15	4	31	23	-23	-10		12	0	24		28	23	-16
7 1	30	13	14	-1	10		9 1	35		20	10	-1	-1	10	9 1	35	31	33	33	33		15	4	32	15	8	12		12	0	25		33	-33	-7
7 1	31	5	29	-18	22		9 1	36		21	36	36	-24	-1	9 1	36	43	45	40	18		15	4	33	12	10	-6		12	0	26		18	11	-14
7 1	32	51	51	46	2		9 1	37		22	30	34	24	8	9 1	37	21	0	21	0		15	4	34	12	10	-6		12	0	27		10	0	-1
7 1	33	80	80	-80	0		9 1	38		23	30	34	8	-22	9 1	38	33	32	27	17		15	4	35	17	14		12	0	28		24	25	28	0
7 1	34	24	24	-0	-29		9 1	39		24	17	-8	15	-9	9 1	39	58	54	54	1		15	4	36	17	14		12	0	29		34	30	-16	
7 1	35	28	13	-9	0		9 1	40		25	17	-8	15	-9	9 1	40	27	36	-27	-24		15	4	37	10	-10	-10		12	0	30		50	50	0
7 1	36	74	77	-68	-33		9 1	41		26	13	-4	15	-4	9 1	41	13	12	-4	15		15	4	38	21	-1		12	0	31		19	18	-6	
7 1	37	4	20	25	15	19	9 1	42		27	7	4	9	9 1	42	10	-8	-5	-16	14		15	4	39	21	-1		12	0	32		23	22	-3	
7 1	38	33	24	-2	23		9 1	43		28	7	4	9	9 1	43	9	9	9	9	9		15	4	40	21	-1		12	0	33		23	22	-3	
7 1	39	62	62	62	62		9 1	44		29	8	14	-7	12	9 1	44	45	44	-10	11		15	4	41	22	15		12	0	34		23	22	-3	
7 1	40	14	8	11	16		9 1	45		30	23	7	22	9 1	45	41	45	44	-10	11		15	4	42	22	15		12	0	35		25	26	9	
7 1	41	7	8	16	16		9 1	46		31	33	35	0	9 1	46	31	37	27	25		15	4	43	22	15		12	0	36		25	26	9	-0	
7 1	42	75	75	-75	-75		9 1	47		32	33	35	0	9 1	47	27	36	-27	-24		15	4	44	22	15		12	0	37		25	26	9	-0	
7 1	43	10	16	-16	2		9 1	48		33	25	13	9	9 1	48	24	28	28	0		15	4	45	22	15		12	0	38		26	26	9	-0	
7 1	44	43	48	48	-1		9 1	49		34	25	13	9	9 1	49	24	28	28	0		15	4	46	22	15		12	0	39		26	26	9	-0	
7 1	45	1	65	63	-23	-9	9 1	50		35	25	13	9	9 1	50	24	28	28	0		15	4	47	22	15		12	0	40		26	26	9	-0	
7 1	46	32	41	46	43	-16	9 1	51		36	25	19	9	9 1	51	24	28	28	0		15	4	48	22	15		12	0	41		26	26	9	-0	
7 1	47	9	37	44	41	-9	9 1	52		37	26	25	7	9 1	52	24	28	28	0		15	4	49	22	15	</									

TABLE 6. Dimensions and Orientations of Thermal Ellipsoids in Pentagonite*

Atom	Rms vib.	Angle to a	Angle to b	Angle to c	Atom	Rms vib.	Angle to a	Angle to b	Angle to c
Ca	0.108(12)	113(13)	90	23(13)	O ₄	0.10(4)	46(78)	123(90)	62(16)
	0.138(8)	90	0	90		0.11(4)	125(84)	144(90)	96(46)
	0.148(11)	23(13)	90	67(13)		0.20(2)	116(10)	78(15)	29(10)
V	0.114(10)	49(9)	90	41(9)	O ₅	0.05(6)	103(15)	83(15)	15(15)
	0.126(8)	90	0	90		0.16(6)	40(90)	50(90)	84(90)
	0.151(8)	139(9)	90	49(9)		0.18(6)	53(90)	140(90)	77(90)
Si ₁	0.083(16)	87(10)	92(14)	3(10)	O ₆	0.14(4)	107(35)	90	17(35)
	0.173(12)	102(27)	168(27)	91(15)		0.18(3)	163(35)	90	107(35)
	0.143(11)	167(26)	78(27)	87(10)		0.21(3)	90	0	90
Si ₂	0.065(21)	35(14)	59(19)	75(12)	O ₇	0.13(4)	71(16)	117(18)	33(9)
	0.100(14)	112(19)	36(19)	117(17)		0.20(3)	129(14)	139(18)	99(18)
	0.134(12)	116(10)	74(15)	32(15)		0.31(3)	135(10)	62(10)	58(8)
O ₁	0.08(4)	108(30)	149(38)	66(26)	O ₈	0.14(6)	54(10)	90	36(10)
	0.12(3)	46(27)	120(39)	122(26)		0.26(5)	90	0	90
	0.18(3)	49(20)	83(16)	42(19)		0.31(5)	144(10)	90	54(10)
O ₂	0.08(5)	115(23)	50(31)	51(36)	O ₉	0.21(6)	170(6)	90	80(6)
	0.13(3)	108(55)	56(48)	141(36)		0.36(7)	90	0	90
	0.15(3)	32(38)	59(41)	88(50)		0.62(11)	80(6)	90	10(6)
O ₃	0.08(3)	144(11)	125(11)	85(10)					
	0.17(2)	125(14)	40(35)	106(78)					
	0.18(2)	95(46)	74(63)	17(74)					

*Principal vibrations (root-mean-square) in Å cited for each atom; angles in degrees. Standard errors indicated in parentheses in terms of last significant figures.

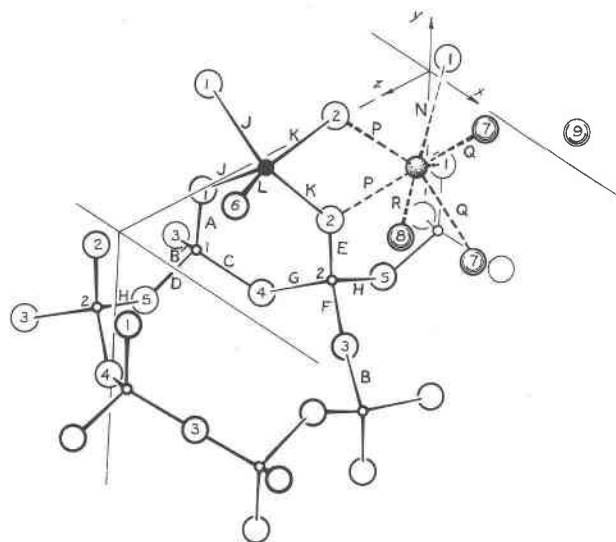


Fig. 2. Bonding configurations in pentagonite. Letters refer to bond vectors listed in Table 7.

4.46 (± 0.11), respectively. If, as Wilhelmi, Waltersson, and Kihlberg (1971) have suggested, a unit V-O bond length of 1.789 Å is assumed instead of 1.81 Å, the valence sums are 4.08 and 4.22 (± 0.11) respectively. This empirical semiquantitative approach merely serves to indicate that the apical bond (in the VO²⁺ group) is mainly a double bond, and that vanadium contributes approximately one-half bond to each silicate link. The remaining charge of -0.5 on these oxygen atoms is just satisfied by the Ca²⁺ ion coordination. As found by Evans and Block (1966) in other structures, in cavansite a sixth oxygen atom O₈ (H₂O) approaches the VO₅ groups at the base of the pyramid, leading to a highly dis-

torted octahedral coordination for vanadium. The sixth distance (2.89Å) is so large that bonding between these atoms must be extremely weak. In pentagonite the nearest approaching oxygen atom (from a neighboring VO²⁺ group) is at an even greater distance (3.25Å).

The only other silicate complex in which VO²⁺ groups play a cross-linking role like that in cavansite

TABLE 7. Interatomic Distances and Bond Angles in Cavansite and Pentagonite

Atoms	Vectors*	Distances and angles**		Atoms	Vectors*	Distances and angles**	
		Cavansite	Pentagonite			Cavansite	Pentagonite
SiO₄ tetrahedra:				VO₅ square pyramids:			
Si ₁ -O ₁	A	1.611(14)	1.589(16)	V-O ₁	J(2x)	1.976(12)	2.000(15)
Si ₁ -O ₂	B	1.633(13)	1.568(19)	V-O ₂	K(2x)	1.973(14)	1.962(15)
Si ₁ -O ₃	C	1.651(13)	1.603(18)	V-O ₆	L	1.597(22)	1.565(27)
Si ₁ -O ₄	D	1.645(15)	1.611(17)	V-O ₈ (H ₂ O)	M	2.887(33)	
Ave		1.635	1.592				
O ₁ -Si ₁ -O ₂	AAB	113.4(8)	112.2(11)	O ₁ -V-O ₆	JAL(2x)	104.6(8)	102.3(8)
O ₁ -Si ₁ -O ₃	AAC	111.5(7)	112.9(8)	O ₂ -V-O ₆	KAL(2x)	104.7(8)	105.3(8)
O ₁ -Si ₁ -O ₄	AAD	113.5(8)	110.8(8)	O ₁ -V-O ₂	JAK(2x)	90.3(6)	91.2(5)
O ₂ -Si ₁ -O ₃	BAC	107.6(7)	108.4(10)	O ₁ -V-O ₁	JAJ	86.6(7)	81.0(9)
O ₂ -Si ₁ -O ₄	BAD	103.3(7)	107.6(9)	O ₂ -V-O ₂	KAK	78.2(9)	83.6(8)
O ₃ -Si ₁ -O ₄	CAD	107.1(7)	104.5(8)				
Ave		109.4	109.4	Ca coordination:			
Si ₂ -O ₂	E	1.613(16)	1.599(16)	Ca-O ₁	N(2x)	2.385(12)	2.407(16)
Si ₂ -O ₃	F	1.611(13)	1.613(19)	Ca-O ₂	P(2x)	2.433(15)	2.342(15)
Si ₂ -O ₄	G	1.630(14)	1.627(18)	Ca-O ₇ (H ₂ O)	Q(2x)	2.392(17)	2.326(18)
Si ₂ -O ₅	H	1.623(15)	1.596(16)	Ca-O ₈ (H ₂ O)	R	2.516(21)	2.465(35)
Ave		1.619	1.608	Ca-O ₉ (H ₂ O)	S	2.844(43)	
				Ave (<2.7)		2.419	2.374
O ₂ -Si ₂ -O ₃	EAF	111.4(8)	112.8(1.2)	Oxygen links:			
O ₂ -Si ₂ -O ₄	EAG	111.2(7)	111.2(8)	Si ₁ -O ₃ -Si ₂	EAF	136.4(8)	176.3(1.6)
O ₂ -Si ₂ -O ₅	EAH	110.8(8)	112.4(8)	Si ₁ -O ₄ -Si ₂	CAG	126.5(9)	131.7(7)
O ₃ -Si ₂ -O ₄	FAG	109.8(7)	105.5(1.1)	Si ₁ -O ₁ -Si ₂	DAH	129.1(9)	140.5(9)
O ₃ -Si ₂ -O ₅	FAH	107.3(7)	108.1(9)	Si ₁ -O ₁ -V	AJ	135.4(7)	132.1(1.0)
O ₄ -Si ₂ -O ₅	GAH	106.2(7)	106.4(8)	Si ₁ -O ₂ -V	EAK	127.9(9)	134.7(9)
Ave		109.5	109.4	Hydrogen bonds (<3.00):			
				O ₇ -O ₁		2.86(2)	
				O ₇ -O ₄			2.96(3)
				O ₇ -O ₈		2.89(4)	
				O ₇ -O ₉		3.00(3)	2.81(3)
				O ₈ -O ₈			2.92(6)
				O ₈ -O ₂			2.98(4)

*Vectors are illustrated in Figs. 1 and 2.
**Distances in Å and angles in degrees, with standard errors indicated in parentheses in terms of last significant figures.

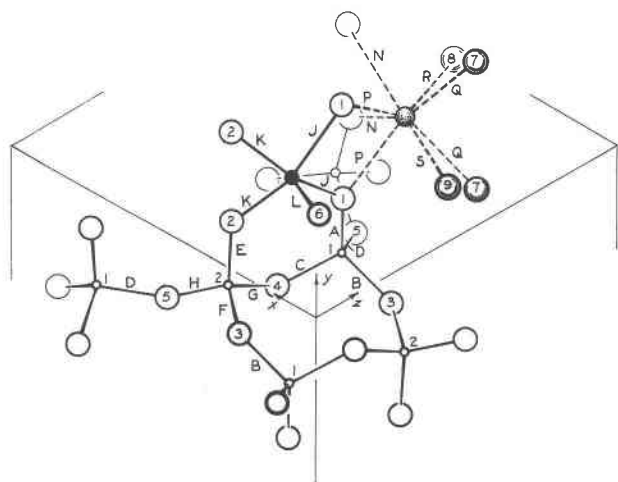


Fig. 1. Bonding configurations in cavansite. Letters refer to bond vectors listed in Table 7.

and pentagonite is found in the mineral haradaite, $\text{Sr}(\text{VO})\text{Si}_2\text{O}_6$. According to the structure analysis of Takeuchi and Joswig (1967), folded $(\text{SiO}_3)_n$ chains are linked laterally by VO^{2+} groups to form a novel vanadosilicate layer. The square pyramid coordination of V^{4+} is very similar to that in our minerals, with an apical V-O bond length of $1.573(5)\text{\AA}$ and four basal bond lengths of $1.99(3)\text{\AA}$.

The calcium ion is coordinated to 4 silicate oxygen atoms, in a manner similar to vanadium in both structures, and to 3 additional water molecules. The configuration is approximately that of a trigonal prism with a seventh H_2O molecule approaching at one prism face. In cavansite, another H_2O molecule stands at a further distance (2.84\AA), encroaching on the coordination sphere; in pentagonite this extra molecule is far removed (3.43\AA). The thermal motion of the H_2O molecules is greater, the further the distance between them and the Ca^{2+} ion. A few rather weak hydrogen bonds apparently prevail between the H_2O molecules and neighboring oxygen atoms (see Table 7).

The Silicate Layer Networks

The outstanding difference between the crystal structures of cavansite and pentagonite is the nature

of the tetrahedral linkages in the silicate layers. Both may be considered as being composed of $(\text{SiO}_3)_n$ chains running parallel to the c axis. Such chains are then linked laterally to adjacent chains to form the sheets, the tetrahedral apices of one chain pointing in opposite directions (along either $+$ or $-b$) from the adjacent chain. The apices in one chain are then coordinated in pairs alternately along the chain with vanadium and calcium in mirror planes between the layers. The lateral linkage of the chains into sheets, however, occurs in such a way that a tessellation of 4- and 8-fold rings is formed in cavansite, while only 6-fold rings are formed in pentagonite. This difference in linkage is illustrated in Figure 3. In spite of this rather drastic shift in linkage, the general crystal chemical and physical properties of the dimorphs are remarkably similar.

The 4-8-fold ring tessellations are fairly common in silicates. Although most layer silicates consist of 6-fold ring linkages, apophyllite and gillespite are two well known layer-structure types that are based on 4-8-fold ring linkages. The 4-8 linkage is more common in framework structures, such as feldspars and zeolites, in which the layers are further linked from sheet to sheet to form three-dimensional networks. Smith and Rinaldi (1962) have made a systematic analysis of the 4-8-fold ring linkages found in framework structures, in terms of the manner in

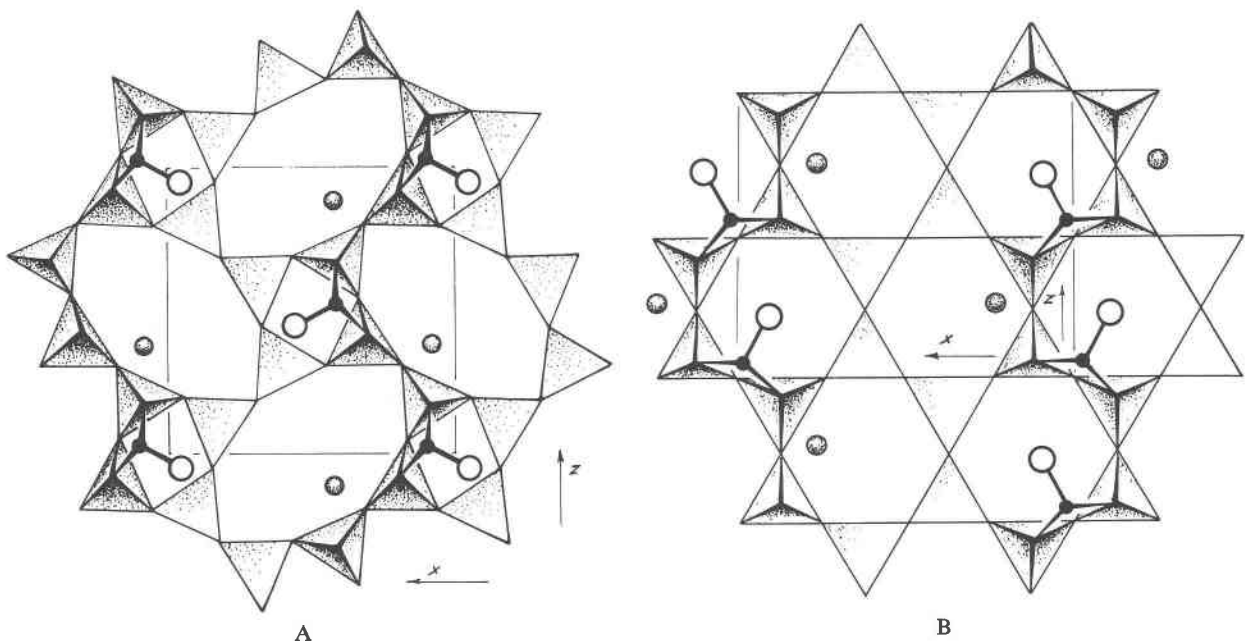


FIG. 3. View along the b axis showing silicate linkages in the crystal structure of (A) cavansite, and (B) pentagonite. Filled circles with attached open circles represent VO^{2+} groups; small shaded circles are Ca^{2+} ions. Water molecules are not shown.

which the tetrahedra in the 4-fold rings are pointed up or down in the layer element. In apophyllite (and gillespite) the tetrahedral apices in each 4-fold ring all point up or all point down, alternating in the layer linkage. This corresponds to the type indicated as Na-Pl in Smith and Rinaldi's Figure 4. In cavansite, the apices point up and down in pairs in the 4-fold rings, as in the type *N* in their Figure 3. The linkage of these rings into layers then produces the zig-zag chains referred to earlier. The postulated assignment of Na-Pl, if it is isostructural with gismondite, was not supported by Fischer's structure analysis of the latter (Fischer, 1963; Fischer and Schramm, 1971).

An interesting analogy can be drawn between cavansite and the zeolite, gismondite. If the VO^{2+} groups are removed and the opposite tetrahedral apices joined directly (subtracting VO_3), and half the Si atoms are replaced by Al, a framework linkage identical topologically with that found by Fischer for gismondite, $\text{CaAl}_2\text{Si}_2\text{O}_8 \cdot 4\text{H}_2\text{O}$, is obtained. One layer from the gismondite structure (Fig. 4) shows tessellation and parallel-linked chains similar to the layer in cavansite (Fig. 3A). However, in gismondite the exposed tetrahedral apices in adjacent layers are linked, not through VO^{2+} groups, but directly to form a three-dimensional aluminosilicate network. In terms of purely layer-type structures, the cavansite linkage appears to be unique.

The layer structures based on 6-fold rings are

generally completely polar, with all tetrahedral apices pointed to the same side of the sheet, as in the micas. In pentagonite each 6-fold ring has one adjacent pair of tetrahedra pointed opposite to the rest; the rings are then linked so that as many point to one side of the sheet as to the other, thus defining the component chains mentioned earlier. Again, this arrangement seems to be unique.

One notable consequence of the shift from a 4-8 linkage to a 6-6 linkage is the appearance in the latter case of a nearly straight Si-O-Si bond configuration. In cavansite all the Si-O-Si and Si-O-V links have angles ranging from 126 to 137° as would be expected, but in pentagonite one of the basal tetrahedral links (at O_3) has an angle of $176.3 \pm 1.6^\circ$ (see Table 7). The root-mean-square amplitude of vibration normal to this oxygen link ($0.18 \pm 0.02 \text{ \AA}$) is not excessive. This linking atom (O_3) lies near the hypothetical symmetry center in the space group *Ccmm* to which the silicate framework closely conforms. Such straight linkages are uncommon, especially where no great amount of disorder is involved. The structure of thortveitite is the best known previous example (Cruikshank, Lynton, and Barclay, 1962). Another example is provided by the previously mentioned vanadosilicate, haradaite (Takeuchi and Joswig, 1967).

The dimorphous structures, cavansite and pentagonite, are, of course, completely incompatible as far as any displacive transition is concerned, and one can only be produced from the other by completely disassembling and reassembling the structure. Both are presumably primary products in mineral genesis, with no evidence of pseudomorphism appearing.

The Role of Water in the Dimorphs

Although no physical chemical studies have been made on cavansite and pentagonite, both are certainly zeolitic in character. The vanadyl groups in both structures join the layers into three-dimensional frameworks that have large channels running parallel to the *c* axis. As shown above, cavansite is very similar to gismondite in this respect. In comparing cavansite and pentagonite, for the former we find 8-fold ring openings allowing passage between the *c*-axis channels in the *b* direction, but in pentagonite these openings are through 6-fold rings and are presumably much more restrictive. Thus, zeolitic migration in cavansite would be three-dimensional, but hardly more than one-dimensional in pentagonite. Nevertheless, the similar unit cell volumes show that

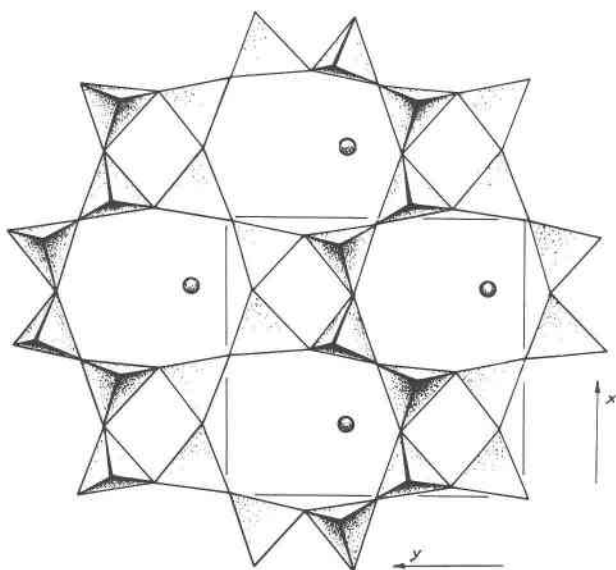


FIG. 4. View of the aluminosilicate layer section in the zeolite gismondite, for comparison with Figure 3(A).

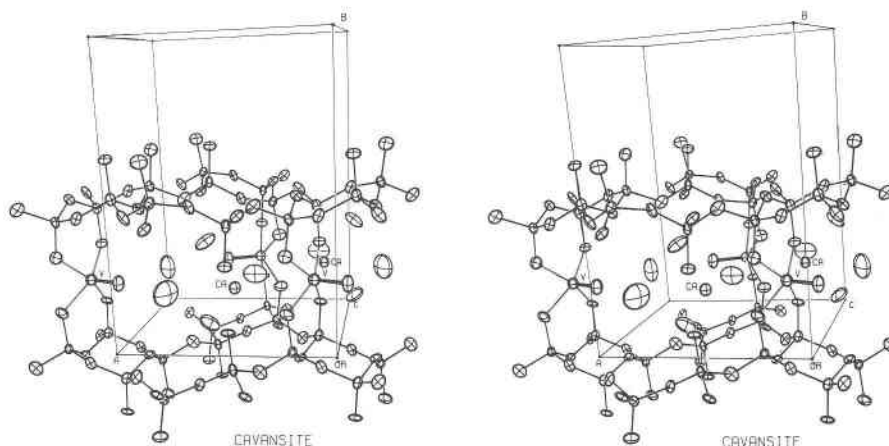


FIG. 5. Stereoscopic view of cavansite, with atoms represented by their 50 percent ellipsoids of vibration. Large, unattached ellipsoids are H_2O molecules.

both structures have equally large cavities, and the structure analysis demonstrates that the H_2O molecules are very loosely bound in both. Thus, the root-mean-square thermal vibrations found for these molecules are of the order of 0.2 to 0.6 Å, and their shapes are extremely anisotropic. The thermal ellipsoids for the H_2O molecules in cavansite and pentagonite (Tables 3 and 6) are oblate spheroids with their short axes aligned approximately toward the Ca^{2+} ions. This effect is clearly apparent in Figures 5 and 6. These cations, however, seem to be firmly attached to the silicate sheets. Additional thermal and structural studies (not presently planned) would be of interest to gain further information concerning the zeolitic behavior of water in these minerals.

Twinning in Pentagonite

Most pentagonite crystals are twinned, while no twins of cavansite have been observed. The twinning

of pentagonite is very characteristic, producing prisms with striking five-pointed, star-shaped cross sections (Staples *et al*, 1973). On twinning by reflection on the (110) plane, the b axis is turned through an angle of 72.68° , so that the internal angles of the pentagon are closely approximated. But the corresponding angle for cavansite would be 71.33° ; therefore, some explanation for the twinning must be sought beyond a possible tendency for pseudo-fivefold symmetry. As a matter of fact, the crystal structures provide a satisfactory understanding of the twinning.

Figure 8 shows the probable composition plane parallel to (110), with a portion of the twin attached. The oxygen atoms in the structure which link the silicate chains together laterally across the composition plane (O_3) actually lie almost exactly on this plane, at $x, y, z = 0.253, 0.247, 0.011$ and $0.247, 0.253, 0.511$. To avoid crowding of the O_5

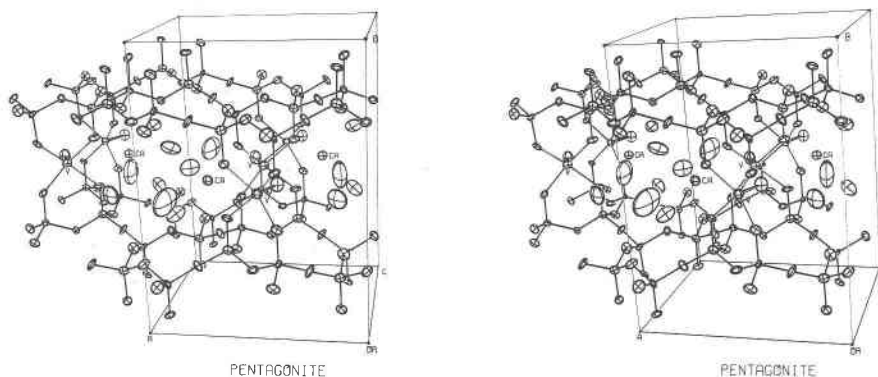


FIG. 6. Stereoscopic view of pentagonite, with atoms represented as in Figure 5.

atoms and permit a more favorable silicate linkage, a $c/2$ glide operation in the composition plane is desirable, and is readily allowed by the rational spacing along z of the linking atoms. Figure 7 shows the same view for cavansite, in which it can be seen that the silicate chain atoms (O_3) that might form twin links are a considerable distance from such a composition plane. Thus, construction of a twin component would involve a large amount of strain in the original structure. The lack of structural integrity across a composition plane is considered to prevent the formation of twins in cavansite, whereas the nearly perfect integrity in pentagonite causes twinning to be almost ubiquitous.

The observation that pentagonite twins are frequently fully developed into fivelings, and that all multiple twins appear to emanate from a common axis, suggests that twinning is initiated in the nucleating process. The structural integrity of pentagonite twinning will extend completely around an imagined nucleating axis parallel to c . This process leads to the formation of concentric prismatic tubes formed from the segments of silicate layers in the twin components, as illustrated in Figure 9. The first tubelike silicate element can be considered as the nucleus which initiates crystal growth. A perspective

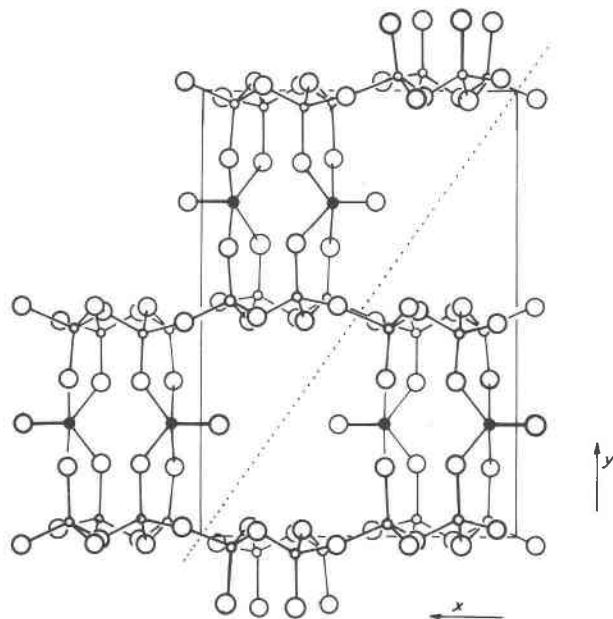


FIG. 7. View along the c axis (showing silicate chains on end) of the crystal structure of cavansite. The dotted line indicates a possible twin composition plane (not so far observed).

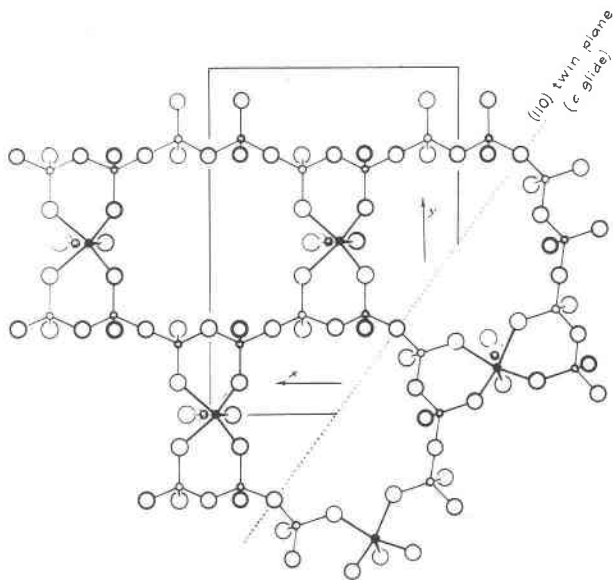


FIG. 8. View along the c axis of pentagonite. A twin component is shown at the right to illustrate the linkage across the (110) twin (composition) plane.

impression of this nucleus is shown in Figure 10. No charges would develop in the interior, which can easily be filled with water molecules. A similar nucleating process based on close packing of spheres has been postulated as the origin of multiple twins with five-fold pseudosymmetry in certain metal crystals (Bagley, 1970; Clarke, 1966).

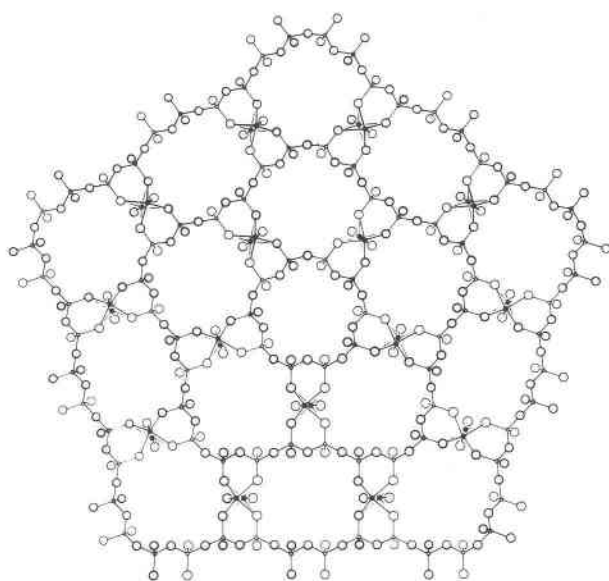


FIG. 9. View of pentagonite similar to Figure 8, but with five equally developed twin components.

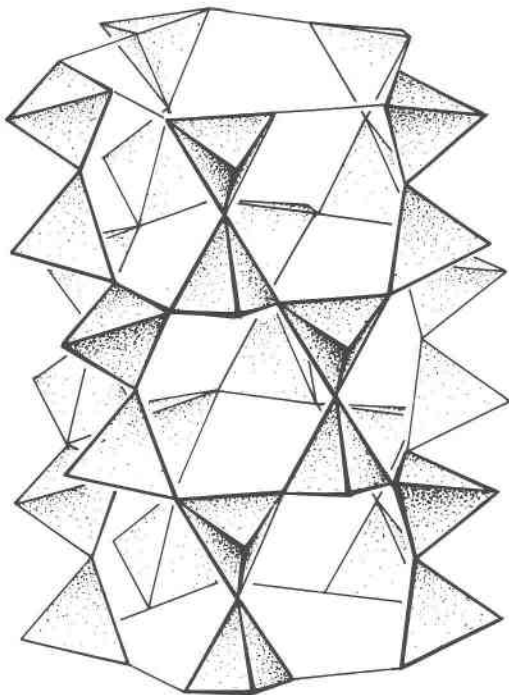


FIG. 10. Perspective view of the silicate tube structure that is supposed to form the nucleus of the pentagonite fiveling.

It was the "aerial" view of the pentagonite structure shown in Figure 9 that actually inspired the name for this mineral. An alternative suggestion that the species be named "redstarite" had to be rejected, among other reasons because the crystals are in fact blue.

References

- BAGLEY, B. G. (1970) Five-fold pseudosymmetry. *Nature*, **225**, 1040-1041.
- BROWN, G. E., AND G. V. GIBBS (1969) Oxygen coordination and the Si-O bond. *Amer. Mineral.* **54**, 1528-1539.
- BURBANK, R. D. (1952) Upper level precession photography and the Lorentz-polarization correction. Part I. *Rev. Sci. Instr.* **23**, 321-327.
- CLARKE, J. A. R. (1966) A dense packing of hard spheres with five-fold symmetry. *Nature*, **211**, 280-281.
- CRUIKSHANK, D. W. J., H. LYNTON, AND G. A. BARKLAY (1962) A reinvestigation of the crystal structure of thortveitite $\text{Sc}_2\text{Si}_2\text{O}_7$. *Acta Crystallogr.* **15**, 491-498.
- EVANS, H. T., JR. (1960) Crystal structure refinement and vanadium bonding in the metavanadates KVO_3 , NH_4VO_3 and $\text{KVO}_3 \cdot \text{H}_2\text{O}$. *Z. Kristallogr.* **114**, 257-277.
- , AND S. BLOCK (1966) Crystal structure of potassium and cesium trivanadates. *Inorg. Chem.* **5**, 1808-1814.
- , AND L. W. STAPLES (1970) The crystal structure of cavansite, a novel layer silicate (abstr). *Geol. Soc. Amer. Abstr. Programs*, **2**, 548.
- FISCHER, K. F. (1963) The crystal structure determination of the zeolite gismondite $\text{CaAl}_2\text{Si}_2\text{O}_8 \cdot 4\text{H}_2\text{O}$. *Amer. Mineral.* **48**, 664-672.
- , AND V. SCHRAMM (1971) Crystal structure of gismondite, a detailed refinement. *Advances in Chemistry Series No.* **101**, 250-258.
- KARLE, J., AND I. L. KARLE (1966) The symbolic addition procedure for phase determination for centrosymmetric and noncentrosymmetric crystals. *Acta Crystallogr.* **21**, 849-859.
- SMITH, J. V., AND F. RINALDI (1962) Framework structures formed from parallel four- and eight-membered rings. *Mineral. Mag.* **33**, 202-212.
- STAPLES, L. W., H. T. EVANS, JR., AND J. R. LINDSEY (1968) Cavansite, a new calcium vanadium silicate mineral. (abstr.) *Geol. Soc. Amer. Spec. Pap.* **115**, 211-212.
- , ———, ——— (1973) Cavansite and pentagonite, new dimorphous calcium vanadium silicate minerals from Oregon. *Amer. Mineral.* **58**, 405-411.
- STEWART, J. M., Ed. (1967) X-RAY 67 program system for X-ray crystallography. *Tech. Rep.* **67-58**, Computer Science Center, University of Maryland.
- TAKEUCHI, Y., AND W. JOSWIG (1967) The structure of haradaite and a note on the Si-O bond lengths in silicates. *Mineral. J.* **5**, 98-123.
- WILHELMI, K.-A., K. WALTERSSON, AND L. KIHLEBORG (1971) A refinement of the crystal structure of V_8O_{18} . *Acta Chem. Scand.* **25**, 2675-2687.

Manuscript received, July 31, 1972; accepted for publication, December 14, 1972.